Subtype-Specific Regulation of Receptor Internalization and Recycling by the Carboxyl-Terminal Domains of the Human A_1 and Rat A_3 Adenosine Receptors: Consequences for Agonist-Stimulated Translocation of Arrestin3†

Gail Ferguson,‡ Kenneth R. Watterson,§ and Timothy M. Palmer*

Molecular Pharmacology Group, Division of Biochemistry and Molecular Biology, Institute of Biomedical and Life Sciences, University of Glasgow, Glasgow G12 8QQ, Scotland, U.K.

Received June 12, 2002; Revised Manuscript Received October 4, 2002

ABSTRACT: In this study, we have characterized the differential effects on inhibitory adenosine receptor (AR) trafficking of disrupting predicted sites for palmitoylation and phosphorylation within each receptor's carboxyl terminus. While a $Cys^{302,305}$Ala-mutated rat A_3AR mutant internalizes significantly faster than the wild-type (WT) receptor in response to agonist exposure, analogous mutation of the human A_1AR (Cys^{309}Ala) had no effect on receptor internalization. Moreover, unlike the WT A_3AR, the entire pool of internalized mutant A_3AR is able to recycle back to the plasma membrane following agonist removal. These properties do not reflect utilization of an alternative trafficking pathway, as internalized WT and mutant A_3ARs both accumulate into transferrin receptor-positive endosomal compartments. However, receptor accumulation into endosomes is dependent upon prior G-protein-coupled receptor kinase (GRK)-mediated phosphorylation of the receptor's carboxyl terminus, as replacement of the carboxyl-terminal domain of the human A_1AR with the 14 GRK-phosphorylated amino acids of the rat A_3AR confers rapid agonist-mediated endosomal accumulation of the resulting chimeric A_1CT3AR. Sensitivity to GRK-mediated phosphorylation also dictates the distinct redistribution of arrestin3 observed upon agonist exposure. Thus, while the nonphosphorylated A_1AR redistributes arrestin3 from the cytoplasm to punctate clusters at the plasma membrane, GRK-phosphorylated WT and $Cys^{302,305}$Ala-mutated A_3ARs, as well as the A_1CT3AR chimera, each induce the redistribution of arrestin3 into punctate accumulations both at the plasma membrane and within the cytoplasm. Neither the human A_1AR nor the rat A_3AR colocalized with arrestin3 under basal or agonist-stimulated conditions. Together, these results demonstrate that inhibitory AR-mediated changes in arrestin3 distribution are subtype-specific, with specificity correlating with the sensitivity of the receptor's carboxyl-terminal domain to GRK phosphorylation. In the case of the rat A_3AR, sensitivity to GRK-mediated internalization appears to be regulated in part by the integrity of putative palmitate attachment sites upstream of its GRK phosphoacceptor sites.

The regulatory effects of extracellular adenosine observed in many tissues are dependent on its ability to bind and activate four distinct adenosine receptor (AR)[1] subtypes, termed A_1, A_{2A}, A_{2B}, and A_3 (*1*). Like almost all G-protein-coupled receptors (GPCRs), each AR protein consists of an extracellular amino-terminal domain linked to a cytoplasmic carboxyl-terminal domain by seven transmembrane-spanning α-helices (*2*). The A_3AR has been demonstrated to play a key role in several important physiological effects of adenosine, including the inhibition of eosinophil activation (*3*) and myocardial protection following sustained periods of hypoxia (*4*).

The rate at which signal output from any given GPCR is terminated, or "desensitized", is typically controlled by its sensitivity to phosphorylation by second messenger-activated kinases and/or G-protein-coupled receptor kinases (GRKs) (*5*). We have shown previously that the distinct rates at which the human A_1- and rat A_3ARs are desensitized are dictated

† Supported by project grants from the British Heart Foundation and Biotechnology and Biological Sciences Research Council, equipment grants from Tenovus-Scotland, the Wellcome Trust, and the National Heart Research Fund, a Medical Research Council Co-operative Group grant in Molecular Genetics and Cellular Signalling in Metabolic and Cardiovascular Syndromes (T.M.P.), and a studentship from the Biotechnology and Biological Sciences Research Council (K.R.W.).

* To whom correspondence should be addressed. Telephone: +44 141 330 4626. Fax: +44 141 330 4620. E-mail: T.Palmer@bio.gla.ac.uk.

‡ Present address: Department of Pharmacology, University of Virginia, P.O. Box 800735, Charlottesville, VA 22908-0735.

§ Present address: Department of Biochemistry and Molecular Biophysics, Commonwealth University of Virginia, Richmond, VA 23298-0614.

[1] Abbreviations: AR, adenosine receptor; A_1CT3AR, chimeric A_1AR mutant in which the carboxyl-terminal domain following Cys309 has been replaced with the 14 carboxyl-terminal amino acids of the rat A_3AR; GRK, G-protein-coupled receptor kinase; GPCR, G-protein-coupled receptor; PKA, cAMP-dependent protein kinase; GFP, green fluorescent protein; [^{125}I]ABMECA, ^{125}I-labeled N^6-(3-iodobenzyl)-5′-*N*-methylcarboxamidoadenosine; DPCPX, dipropylcyclopentylxanthine; MRS1523, 5-propyl 2-ethyl-4-propyl-3-(ethylsulfanylcarbonyl)-6-phenylpyridine-5-carboxylate; R-PIA, (*R*)-N^6-(phenylisopropyl)adenosine; TRH, thyrotropin-releasing hormone; HA, hemagglutinin; WT, wild-type; CHO, Chinese hamster ovary; HEK293, human embryonic kidney 293; PBS, phosphate-buffered saline; PBSGG, PBS supplemented with 0.1% (v/v) goat serum and 0.2% (w/v) gelatin; VSV, vesicular stomatitis virus.

10.1021/bi0262911 CCC: $22.00
Published on Web 11/20/2002

by structural differences in their cytoplasmic carboxyl-terminal domains (*6*). Specifically, rapid functional desensitization of the rat A_3AR occurs within minutes of agonist exposure and is associated with the phosphorylation of specific carboxyl-terminal threonine residues by one or more GRK family members (*6*−*8*). In contrast, the slowly desensitizing human A_1AR is not phosphorylated in response to agonist exposure, and is desensitized only after agonist exposure for several hours or even days (*9*−*11*). In addition, we have recently made the novel observation that agonist-occupied human A_1- and rat A_3ARs each internalize over distinct time courses and that the kinetics of receptor internalization are also determined by each receptor's sensitivity to phosphorylation by GRKs (*9*).

In common with many GPCRs, the A_1- and A_3ARs each have conserved Cys residues present within their cytoplasmic carboxyl-terminal domains. On the basis of studies performed predominantly with rhodopsin and the β_2-adrenergic receptor, these residues are presumed to be sites for post-translational attachment of palmitate, an event which is thought to anchor the carboxyl-terminal tail to the plasma membrane to form a fourth intracellular loop (*12*). However, it is now appreciated that palmitoylation is a dynamic process influenced by agonist occupation of the receptor protein. In the case of the β_2-adrenergic receptor, it has been proposed that changes in receptor palmitoylation status regulate its ability to undergo phosphorylation by cAMP-dependent protein kinase (PKA) and GRK2 (*13*, *14*). Specifically, removal of palmitate from Cys341 within the receptor's carboxyl-terminal tail by either agonist pretreatment or mutation of Cys341 to Ala increases the degree of β_2-adrenergic receptor phosphorylation on a consensus PKA site at Ser346. In addition, phosphorylation of this site enhances agonist-dependent GRK2-dependent phosphorylation of the receptor downstream of the site of palmitate attachment (*14*). The resulting increase in the degree of receptor phosphorylation uncouples the receptor from G_s, thus inhibiting adenylyl cyclase activation (*13*, *14*). Consistent with these observations, we have demonstrated that a mutant A_3AR in which two potential sites for palmitate attachment in the carboxyl-terminal tail (Cys302 and -305) have been disrupted displays a significant agonist-independent basal phosphorylation, unlike the WT receptor (*7*). Although these observations might suggest a role for palmitate turnover in controlling the accessibility of the carboxyl-terminal domains of the A_3AR and β_2-adrenergic receptors to specific regulatory kinases, this is clearly not universally applicable as disruption of analogous carboxyl-terminal Cys residues has no effect on either the phosphorylation status or function of other GPCRs (*15*, *16*).

In this study, we have employed both epitope- and green fluorescent protein (GFP)-tagged forms of the human A_1- and rat A_3ARs to examine the role of potential sites for palmitate attachment in controlling agonist-stimulated changes in the subcellular trafficking of these inhibitory AR subtypes. Via these approaches, we demonstrate that these sites play a key role in specifically controlling the internalization and recycling rates of agonist-occupied A_3ARs but not A_1ARs. In addition, we propose that agonist-stimulated phosphorylation of the A_3AR within its carboxyl-terminal domain dictates the receptor-specific redistribution of arrestin3.

EXPERIMENTAL PROCEDURES

Materials. All tissue culture reagents and R-PIA were from Sigma. Radiochemicals were purchased from either DuPont-NEN or ICN. [^{125}I]ABMECA (2200 Ci/mmol) was synthesized and purified to homogeneity by high-performance liquid chromatography as described previously (*17*). The A_3AR agonist IBMECA and rat A_3AR-selective antagonist MRS1523 were donated generously by K. Jacobson (National Institutes of Health, Bethesda, MD). A mutant HA epitope-tagged Cys^{309}Ala human A_1AR cDNA was the generous gift of M. Olah (University of Cincinnati College of Medicine, Cincinnati, OH). Bovine GRK2 and arrestin3−GFP cDNA expression constructs were generously donated by J. Benovic (Jefferson University, Philadelphia, PA). A VSV epitope-tagged human thyrotropin-releasing hormone (TRH) receptor cDNA was generously donated by G. Milligan (University of Glasgow). Anti-HA antibody 12CA5 and anti-VSV antibody P5D4 were from Roche Diagnostics Ltd. Anti-GFP antibodies were from Clontech. Lipofectamine and OptiMEM were from Life Technologies. Alexa594-conjugated forms of human transferrin and goat anti-mouse IgG were from Molecular Probes. The sources of all other materials have been described elsewhere (*7*, *9*).

Cell Culture and Transfections. The generation and characterization of CHO cell lines stably expressing HA epitope-tagged wild-type (WT), Cys^{302,305}Ala, and Thr^{307,318,319}Ala mutant rat A_3ARs have been described previously by us (*7*, *8*). The CHO cell line expressing the HA epitope-tagged WT human A_1AR has also been characterized previously (*6*). CHO cell lines stably expressing WT A_1AR−GFP and A_3AR−GFP chimeras were generated using a modified calcium phosphate precipitation/glycerol shock procedure as described previously (*8*). Positive clones were identified by fluorescence microscopy and expanded for further study. All CHO cells were maintained in Ham's F-12 medium supplemented with 10% (v/v) fetal bovine serum, 1 mM L-glutamine, 100 units/mL penicillin, and 100 μg/mL streptomycin at 37 °C in a humidified atmosphere containing 5% (v/v) CO_2. Stably transfected clones were maintained in medium supplemented with 0.4 mg/mL G418 to maintain selection pressure. Human embryonic kidney 293 (HEK293) and COS-P cells were grown in Dulbecco's modified Eagle's medium supplemented with fetal bovine serum, L-glutamine, penicillin, and streptomycin.

For transient transfections, HEK293 and CHO cells at approximately 80% confluence plated in six-well dishes were incubated for 3 h in 1 mL/well OptiMEM containing 2 μg of cDNA and 4 μL of Lipofectamine according to the manufacturer's instructions. COS-P cells in 100 mm dishes were transfected with 20 μg of cDNA/dish using a DEAE-dextran protocol that we have described previously (*18*). All cells were used for analysis 36−48 h after transfection.

Generation of Expression Constructs Encoding AR−GFP Chimeras. (1) Rat A_3AR−GFP Constructs. These were each generated by PCR by employing previously described pCMV5/HA epitope-tagged WT, Cys^{302,305}Ala, and Thr^{307,318,319}Ala-mutated A_3AR cDNAs as templates (*7*, *8*). In each case, the primer sequences were 5′-TGATT**AAGCT-T**CCACC*ATG*AAAGCCAACAATACCACGAC-3′ (sense) and 5′-TGATT**CCCGGG**CAGCGTAGTCTGGGACGTC-3′ (antisense). The sense primer was designed to remove the

amino-terminal HA epitope tag sequence and add a *Hin*dIII site (bold) upstream of a consensus Kozak sequence (underlined) and the A_3AR initiating Met (italic). The antisense primer was designed to remove the A_3AR stop codon and add a *Sma*I site (bold). This was to allow in-frame fusion of the carboxyl-terminally HA epitope-tagged A_3AR open reading frames with that of GFP following subcloning of the *Hin*dIII- and *Sma*I-digested PCR products with a similarly digested modified pEGFP-N1 cDNA (Clontech) in which the initiating Met of the GFP open reading frame was mutated to Ala.

(2) Human A_1AR−GFP and A_1CT3AR−GFP Constructs. The A_1AR−GFP chimeras were also each generated by PCR using pCMV5/HA epitope-tagged WT and Cys^{309}Ala human A_1AR cDNAs in combination with the primers 5′-ATTTG-**GAATTC**CCACC*ATG*CCGCCCTCCATCTCAGC-3′ (sense) and 5′-ATTTG**GGTACC**GCAGCGTAGTCTGGGAC-3′ (antisense). The sense primer was designed to remove the amino-terminal HA epitope tag sequence and add an *Eco*RI site (bold) upstream of a consensus Kozak sequence (underlined) and the A_1AR initiating Met (italic). The antisense primer was designed to remove the A_1AR stop codon and add an *Xba*I site (bold). As described for the A_3AR−GFP chimera, this allowed in-frame fusion of the carboxyl-terminally HA epitope-tagged A_1AR open reading frames with GFP following subcloning of the *Eco*RI- and *Xba*I-digested PCR products with the similarly digested modified pEGFP-N1 cDNA. The A_1CT3AR−GFP chimera was generated by PCR using the amino-terminal A_1AR sense primer and the carboxyl-terminal A_3AR antisense primer. The resulting product was digested with *Eco*RI and *Sma*I prior to being subcloned into the modified pEGFP-N1 vector.

The integrity of each receptor−GFP chimera was verified by DNA sequencing.

Receptor Internalization Assay. This was performed using a sequential cell surface biotinylation−immunoprecipitation protocol as described previously by us (*9*). Confluent stably transfected CHO cells in six-well dishes were washed and incubated at 37 °C with normal medium supplemented with 1 unit/mL adenosine deaminase and either vehicle or R-PIA as indicated in the figure legends. For reversal experiments, agonist-containing medium was removed and cell monolayers were washed once with prewarmed medium prior to the addition of fresh medium supplemented with 1 μM MRS1523 at 37 °C for the times indicated in the figure legends. Reactions were terminated by placing the cells on ice, removing the medium, and washing the monolayers twice with ice-cold phosphate-buffered saline (PBS). All subsequent procedures were performed at 4 °C unless indicated otherwise. First, cell surface glycoproteins were conjugated with biotin by sequential incubation with sodium periodate and biotin hydrazide. Cells were then solubilized by scraping them into 0.5 mL of immunoprecipitation buffer [50 mM sodium HEPES (pH 7.5), 150 mM sodium chloride, 5 mM EDTA, 10 mM sodium fluoride, 10 mM sodium phosphate, 1% (v/v) Triton X-100, 0.5% (w/v) sodium deoxycholate, 0.1% (w/v) SDS, 0.1 mM phenylmethanesulfonyl fluoride, 10 μg/mL soybean trypsin inhibitor, and 10 μg/mL benzamidine] and rotating them for 1 h. Following removal of insoluble material by centrifugation, soluble extracts were equalized for protein content and receptors immunoprecipitated by overnight incubation with 1 μg of 12CA5 and 20 μL of 50% (v/v) protein A−Sepharose beads in the presence of 0.2% (w/v) immunoglobulin-free bovine serum albumin. Immune complexes were isolated by brief centrifugation, washed three times with immunoprecipitation buffer, and eluted from the beads by the addition of electrophoresis sample buffer. After fractionation of immunoprecipitated receptors by SDS−PAGE, resolved proteins were transferred to a nitrocellulose membrane. Biotin-labeled immunoprecipitated receptors were then identified by probing blots with horseradish peroxidase-conjugated streptavidin prior to visualization by enhanced chemiluminescence. Quantitation was by densitometric scanning of exposed blots.

Intact Cell Receptor Phosphorylation. These were performed as described previously (*7*). Briefly, confluent CHO cells in six-well dishes were incubated for 90 min with phosphate-free Dulbecco's modified Eagle's medium supplemented with 0.2 mCi/mL of [^{32}P]orthophosphate. Following stimulation with R-PIA as indicated in the figure legends, reactions were terminated by placing cells on ice and washing the monolayers twice with ice-cold PBS. Cells were then solubilized and processed for receptor immunoprecipitation by incubation with 12CA5 and protein A−Sepharose beads for 2 h. Following washing with immunoprecipitation buffer and elution of immunoprecipitated receptors with electrophoresis sample buffer, immunoprecipitates were fractionated by SDS−PAGE and phosphorylated proteins visualized by autoradiography.

Immunoblotting. Transiently transfected CHO cells plated in six-well dishes were washed in PBS and solubilized in 0.25 mL of immunoprecipitation buffer/well. Following rotation for 1 h at 4 °C, soluble extracts were prepared by centrifugation at 14000*g* for 15 min. Samples equalized for protein content were then prepared for SDS−PAGE and immunoblotting with an anti-GFP primary antibody (1:1000 dilution) as described previously (*18*).

Radioligand Binding. Saturation binding experiments using [^{3}H]DPCPX and [^{125}I]ABMECA were performed on membranes prepared from transfected COS-P cells and analyzed as described previously using Graphpad Prism software (*17*).

Confocal Microscopy. Real-time visualization of agonist-stimulated changes in AR−GFP trafficking in transiently transfected CHO cells was performed on cells grown on glass coverslips and manipulated on a heated (37 °C) stage using a Zeiss AxioVERT 100 laser-scanning confocal microscope. Images were collected sequentially from single-line excitation by a 488 nm argon/krypton laser and detected using a 515−540 nm band-pass filter.

Assessment of the colocalization of AR−GFP chimeras with transferrin receptors was performed on transiently transfected HEK293 cells preincubated in serum-free medium containing Alexa594-conjugated human transferrin for 30 min at 37 °C prior to the addition of R-PIA as described in the figure legends. Cells were then washed following agonist treatment, fixed in paraformaldehyde, and mounted onto microscope slides with 40% (v/v) glycerol in PBS for imaging by confocal microscopy using dual excitation (488 and 543 nm) and emission (515−540 nm for GFP and 590−610 nm for Alexa594) filter sets.

For assessment of the colocalization of the arrestin3−GFP chimera with HA- or VSV epitope-tagged receptors, paraformaldehyde-fixed transfected cells plated on coverslips were permeabilized in 0.4% (v/v) Triton X-100 in PBS for 3 min

followed by washing with PBS supplemented with 0.1% (v/v) goat serum and 0.2% (w/v) gelatin (PBSGG) and incubation for 60 min at room temperature with either a 1:200 dilution of anti-HA antibody 12CA5 or anti-VSV antibody P5D4 in PBSGG. Following being washed for 5 min with three changes each of PBSGG and PBS, coverslips were incubated with a 1:200 dilution of Alexa594-conjugated goat anti-mouse IgG for 60 min at room temperature. Coverslips were then washed sequentially in PBSGG and PBS as described above prior to being mounted onto microscope slides with glycerol and PBS for dual-label confocal analysis using the settings described above for detection of GFP- and Alexa594-derived fluorescence. For all dual-labeling experiments, singly labeled controls were routinely included to exclude the possibility of any bleed-through between red and green channels contributing to the observed colocalization. All collected images were analyzed using Metamorph software.

RESULTS

Internalization and Recycling Kinetics of a Cys^{302,305}Ala Mutant A$_3$AR. We have noted previously that mutation of the Cys residues present in the carboxyl-terminal tail of the A$_3$AR to Ala produces a receptor that exhibits significant phosphorylation in the absence of agonist (*7*). Given that the rapid rate of agonist-stimulated A$_3$AR internalization is critically dependent on the ability of the A$_3$AR carboxyl terminus to serve as a GRK substrate (*9*), it was possible that the basal phosphorylation state of the Cys^{302,305}Ala mutant had consequences for receptor internalization. To test this hypothesis, rates of WT and mutant A$_3$AR internalization were compared in response to a maximally effective concentration of the AR agonist R-PIA. Receptor expression levels in the cell lines for which data are presented, as determined by [^{125}I]ABMECA saturation binding analyses, were 0.95 ± 0.24 and 0.36 ± 0.05 pmol/mg of membrane protein for WT and Cys^{302,305}Ala, respectively. A 30 min agonist treatment produced similar maximal reductions in the cell surface level of both receptors [WT reduction = 78 ± 8% vs mutant reduction = 86 ± 6% ($p > 0.05$ NS); Figure 1]. However, the rate at which the Cys^{302,305}Ala mutant A$_3$AR was lost from the cell surface was consistently greater than that observed for the WT A$_3$AR ($t_{1/2}^{WT} = 10$ min, $t_{1/2}^{mutant} = 4$ min, Figure 1). Thus, after a 5 min agonist exposure, 59 ± 6% of the Cys^{302,305}Ala A$_3$AR is lost from the cell surface whereas only 20 ± 12% of the WT receptor has been removed ($p < 0.05$ between the WT and Cys^{302,305}Ala A$_3$AR at 5 min). Similar results were obtained for two separate receptor-expressing clones (data not shown), suggesting that the differences observed were not clonal artifacts.

Receptor recycling back to the plasma membrane is essential for restoring, or "resensitizing", cellular responsiveness following agonist removal. In several instances, resensitization is associated with the dephosphorylation of internalized receptors prior to the recycling event (*19*−*21*). To assess a potential role for the predicted palmitoylation sites within the carboxyl-terminal tail of the A$_3$AR in controlling receptor recycling, the recovery of WT and mutant A$_3$AR expression at the cell surface over time was quantitated following a 30 min agonist exposure and subsequent wash-out (Figure 2). After removal of agonist for 30 min, only 49 ± 11% of the internalized WT A$_3$ARs had recycled back to the cell surface (Figure 2). In contrast, approximately 94 ± 5% of the internalized Cys^{302,305}Ala A$_3$ARs had returned to the plasma membrane ($p < 0.05$ vs recovery of the WT A$_3$AR; Figure 2). Cell surface levels of the WT A$_3$AR only returned to their original levels after incubation for 2 h in agonist-free medium (data not shown). Thus, the presence of Cys residues within the carboxyl-terminal domain of the A$_3$AR, upstream of the receptor's GRK phosphorylation sites, is not only an important determinant of the rates of agonist-stimulated sequestration but also the rate at which cell surface A$_3$AR levels are restored following agonist removal. Again, similar results were obtained for two separate receptor-expressing clones (data not shown), thereby ruling out any possibility that the observed differences were clonal artifacts.

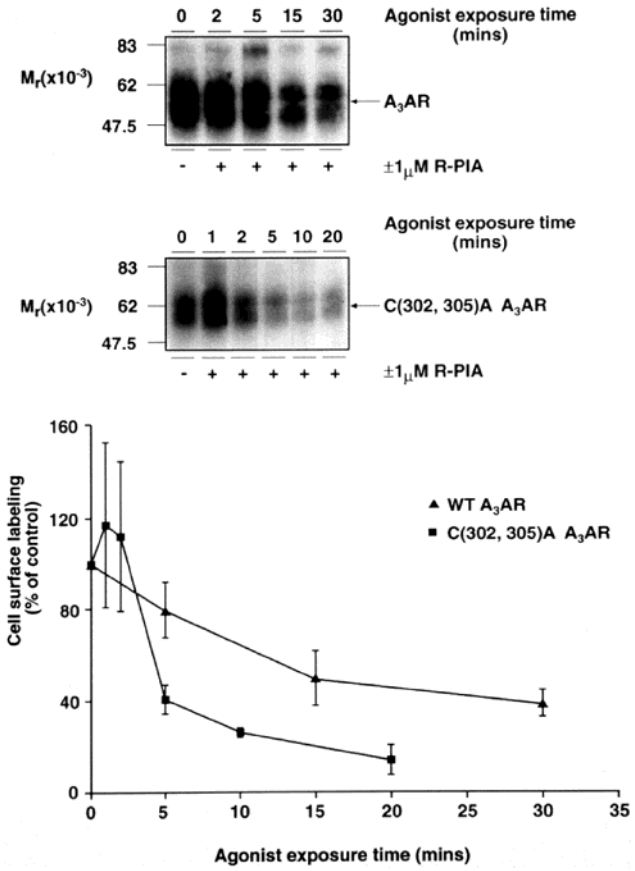

FIGURE 1: Comparative analysis of the time courses of R-PIA-stimulated internalization of WT and Cys^{302,305}Ala-mutated A$_3$ARs. CHO cells stably expressing either HA epitope-tagged WT or Cys^{302,305}Ala-mutated A$_3$ARs were treated with or without 1 μM R-PIA for the indicated times prior to analysis of cell surface A$_3$AR levels by labeling of surface glycoproteins with biotin hydrazide and receptor immunoprecipitation with 12CA5. Following SDS−PAGE and transfer to nitrocellulose, cell surface A$_3$ARs were visualized by probing blots with peroxidase-conjugated streptavidin. Blots show the result from one experiment that was representative of three that were performed. Quantitative analysis from these three experiments is shown.

Expression and Characterization of a WT A$_3$AR−*GFP Chimera.* To visualize the impact of disrupting Cys302 and -305 on the cellular trafficking of the A$_3$AR in single cells, a series of WT and mutant A$_3$AR−GFP chimeras were generated as described in Experimental Procedures. Saturation radioligand binding assays using [^{125}I]ABMECA demonstrated that WT and GFP-tagged A$_3$ARs were expressed

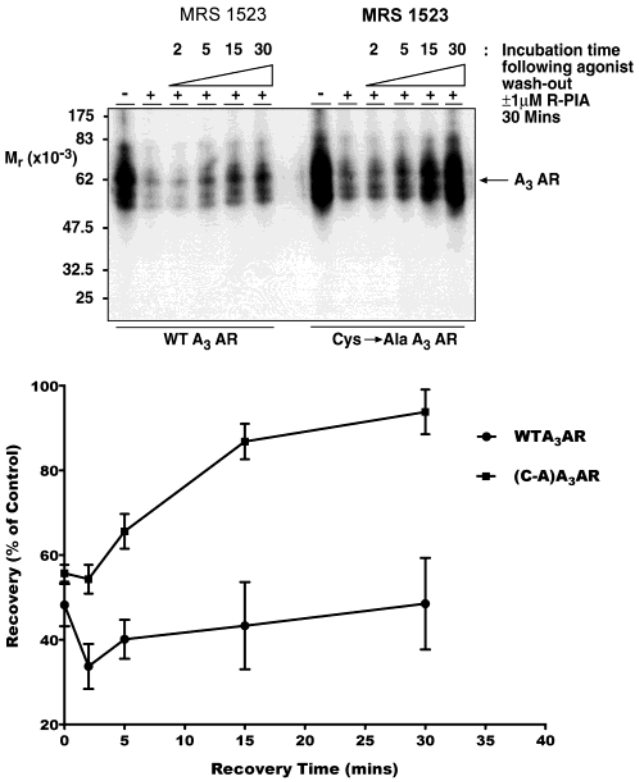

FIGURE 2: Comparative analysis of the time courses of WT and Cys[302,305]Ala-mutated A_3AR recovery to the cell surface following agonist removal. CHO cells stably expressing either HA epitope-tagged WT or Cys[302,305]Ala-mutated A_3ARs were treated with or without 1 μM R-PIA for 30 min to induce receptor internalization. Monolayers were then washed twice to remove agonist, and subsequently incubated for the indicated times in fresh medium supplemented with 1 μM MRS1523, an A_3AR-selective antagonist ligand. After the indicated times, the recovery of A_3ARs to the cell surface was determined by biotinylation of cell surface glycoproteins and receptor immunoprecipitation with 12CA5 as described in Experimental Procedures. Quantitative analysis from three experiments is shown.

at similar levels and displayed K_ds for each radioligand that were both indistinguishable from the values obtained for the non-GFP-tagged receptors (Figure 3A and Table 1) and identical to those obtained by other investigators (*17*). Moreover, cell surface biotinylation assays demonstrated that GFP-tagged A_3ARs are appropriately glycosylated and expressed on the cell surface upon stable expression in CHO cells (Figure 3B).

It has been reported previously that addition of residues to the extreme carboxyl terminus of the β_2-adrenergic receptor has profound effects on its regulation due to the disruption of a PDZ domain binding motif (*22*). While the A_3AR does not possess a similar motif, it was nevertheless important to assess whether the addition of GFP to the receptor's carboxyl terminus altered its sensitivity to agonist-stimulated phosphorylation. In ^{32}P-labeled CHO cells stably expressing either the WT A_3AR or the A_3AR−GFP chimera, preincubation with agonist for 10 min produced similar fold-increases in the phosphorylation status of both receptors (Figure 3C), suggesting that A_3AR sensitivity to agonist-stimulated phosphorylation is not compromised upon fusion of GFP to its carboxyl terminus.

Comparison of the Effects of Phosphorylation and Palmitoylation Site Disruption on A_3AR−GFP Trafficking. To

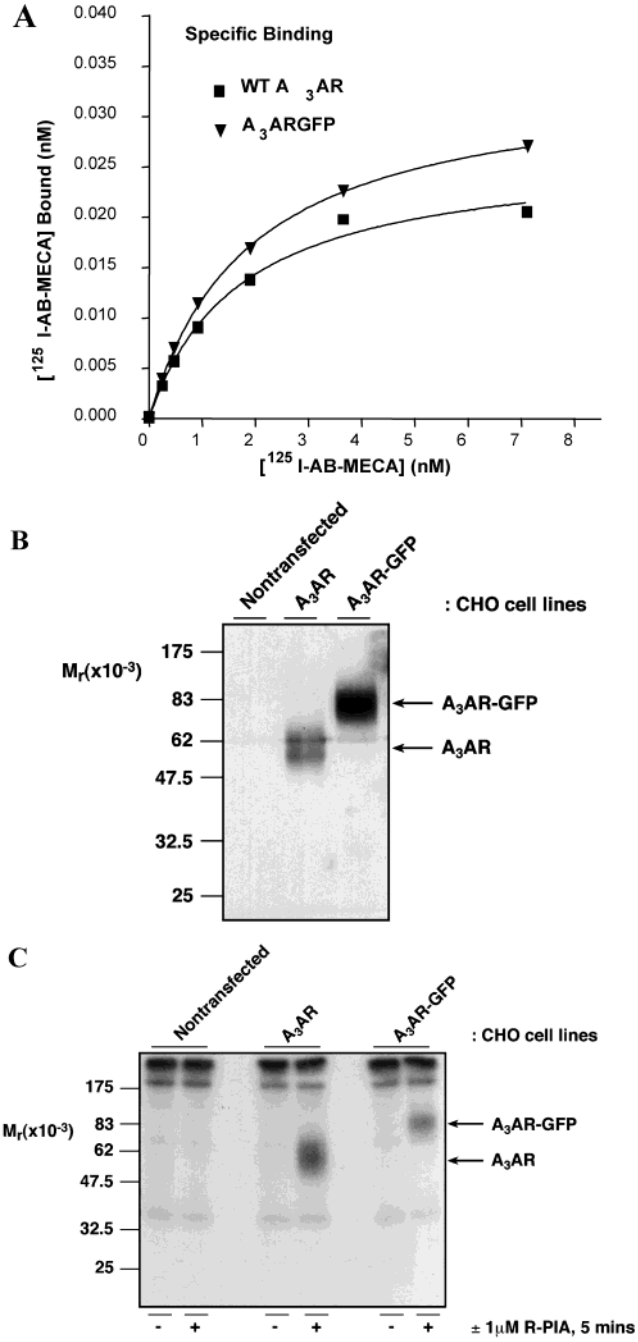

FIGURE 3: Functional analysis of a WT A_3AR−GFP chimera. (A) Membranes prepared from COS-P cells transiently transfected with either WT A_3AR or WT A_3AR−GFP expression constructs were used for saturation radioligand binding assays with increasing concentrations of the A_3AR agonist radioligand [^{125}I]ABMECA as described in Experimental Procedures. This is one of three experiments, composite data from which are presented in the Results. (B) Monolayers of nontransfected CHO cells and CHO cells expressing either an HA epitope-tagged WT A_3AR or a WT A_3AR−GFP chimera were subjected to cell surface biotinylation and receptor immunoprecipitation with 12CA5 as described in Experimental Procedures. Biotinylated receptors were visualized by being transferred to nitrocellulose following SDS−PAGE and probing with peroxidase-conjugated streptavidin. This is one of multiple experiments. (C) Monolayers of nontransfected CHO cells and CHO cells stably expressing either an HA epitope-tagged WT A_3AR or a WT A_3AR−GFP chimera were preincubated with ^{32}P-containing medium prior to stimulation with or without R-PIA as indicated. Following receptor immunoprecipitation with 12CA5, phosphoproteins were visualized by autoradiography. This is one of three experiments that produced identical results.

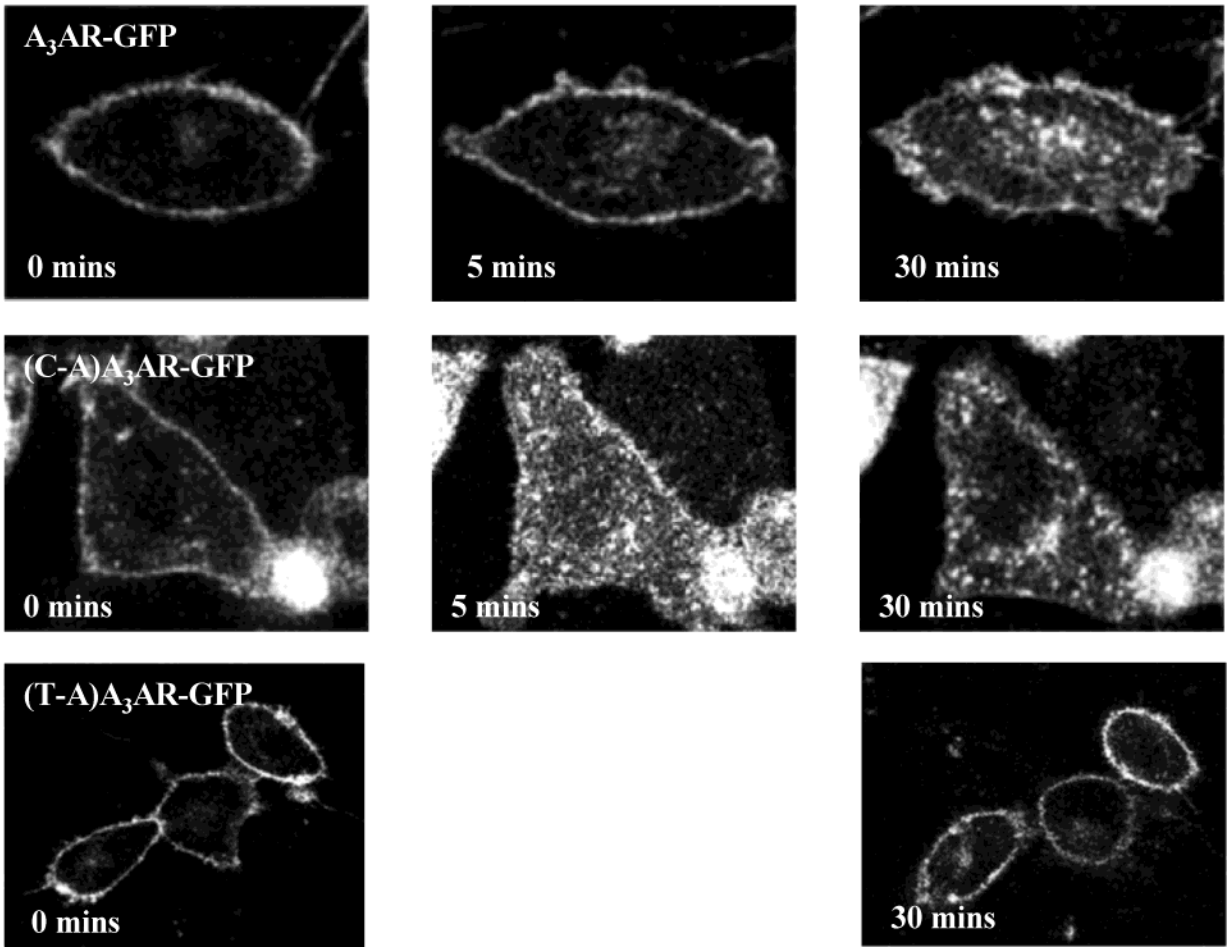

FIGURE 4: Real-time analysis of agonist stimulation of WT and mutant A_3AR−GFP trafficking. CHO cells were transiently transfected with plasmids encoding either WT, $Cys^{302,305}$Ala, or $Thr^{307,318,319}$Ala A_3AR−GFP proteins. The subcellular distribution of receptor−GFP fluorescence was visualized before and after the addition of 1 μM R-PIA at the indicated times. Confocal images of representative cells are shown from a single experiment which was performed multiple times with identical results.

Table 1: Pharmacological Characterization of A_1AR−GFP and A_3AR−GFP Chimeras[a]

receptor	K_d (nM)	B_{max} (pmol/mg of protein)
A_1AR	2.75 ± 0.11	5.32 ± 1.09
A_1AR−GFP	2.29 ± 0.39	3.98 ± 0.52
A_3AR	2.18 ± 0.54	1.20 ± 0.30
A_3AR−GFP	2.03 ± 0.31	1.43 ± 0.20

[a] Membranes prepared from COS-P cells transiently expressing the indicated ARs were used for saturation radioligand binding assays employing increasing concentrations of either the A_1AR-selective antagonist ligand [^{3}H]DPCPX (for the A_1AR and the A_1AR−GFP chimera) or the A_3AR-selective agonist radioligand [^{125}I]ABMECA (for the A_3AR and the A_3AR−GFP chimera) as described in Experimental Procedures. Results are presented as means ± standard error from three experiments.

be a useful tool for studying the dynamics of receptor trafficking, disruption of key regulatory sites within the A_3AR−GFP chimera should produce the same changes that were observed for the corresponding non-GFP-tagged receptor. To test this, two mutant A_3AR−GFP chimeras were generated: one in which each of the GRK phosphorylation sites at Thr307, -318, and -319 was mutated to Ala and another using the $Cys^{302,305}$Ala mutant receptor (*7*). Following expression in CHO cells, agonist-stimulated changes in receptor trafficking were visualized in living cells in real time using confocal microscopy (Figure 4). Consistent with the biochemical data obtained from biotinylation experiments (Figure 1), pretreatment with agonist for 30 min resulted in a profound loss of receptor from the plasma membrane and the parallel accumulation of receptor fluorescence in punctate intracellular vesicles (Figure 4). In contrast, the nonphosphorylated $Thr^{307,318,319}$Ala A_3AR−GFP chimera remained at the cell surface over a 30 min agonist incubation (Figure 4), reflecting the lack of mutant receptor internalization observed in biotinylation assays (*9*). In the case of the Cys-mutated A_3AR−GFP chimera, significant punctate intracellular staining could be detected as early as 5 min following agonist addition, a time point at which internalization of the WT A_3AR−GFP chimera was not yet detectable (Figures 1 and 4). However, as for the WT A_3AR−GFP chimera, accumulation of the Cys-mutated receptor in these vesicles was maximal by 30 min (Figure 4).

Effect of Predicted Palmitoylation Site Disruption on A_1AR−GFP Trafficking. We and others have demonstrated that, in contrast to the rapid phosphorylation and internalization of the A_3AR, the A_1AR is only weakly phosphorylated (*6*, *9*, *11*) and takes several hours to be lost from the cell surface (*9*, *11*, *23*). To determine if the effect of putative palmitoylation site disruption was receptor-specific, two human A_1AR−GFP chimeras were generated: one containing the WT A_1AR and another encoding a mutant human A_1AR in which Cys309 in the carboxyl-terminal domain was mutated to Ala. This mutation has been shown previously

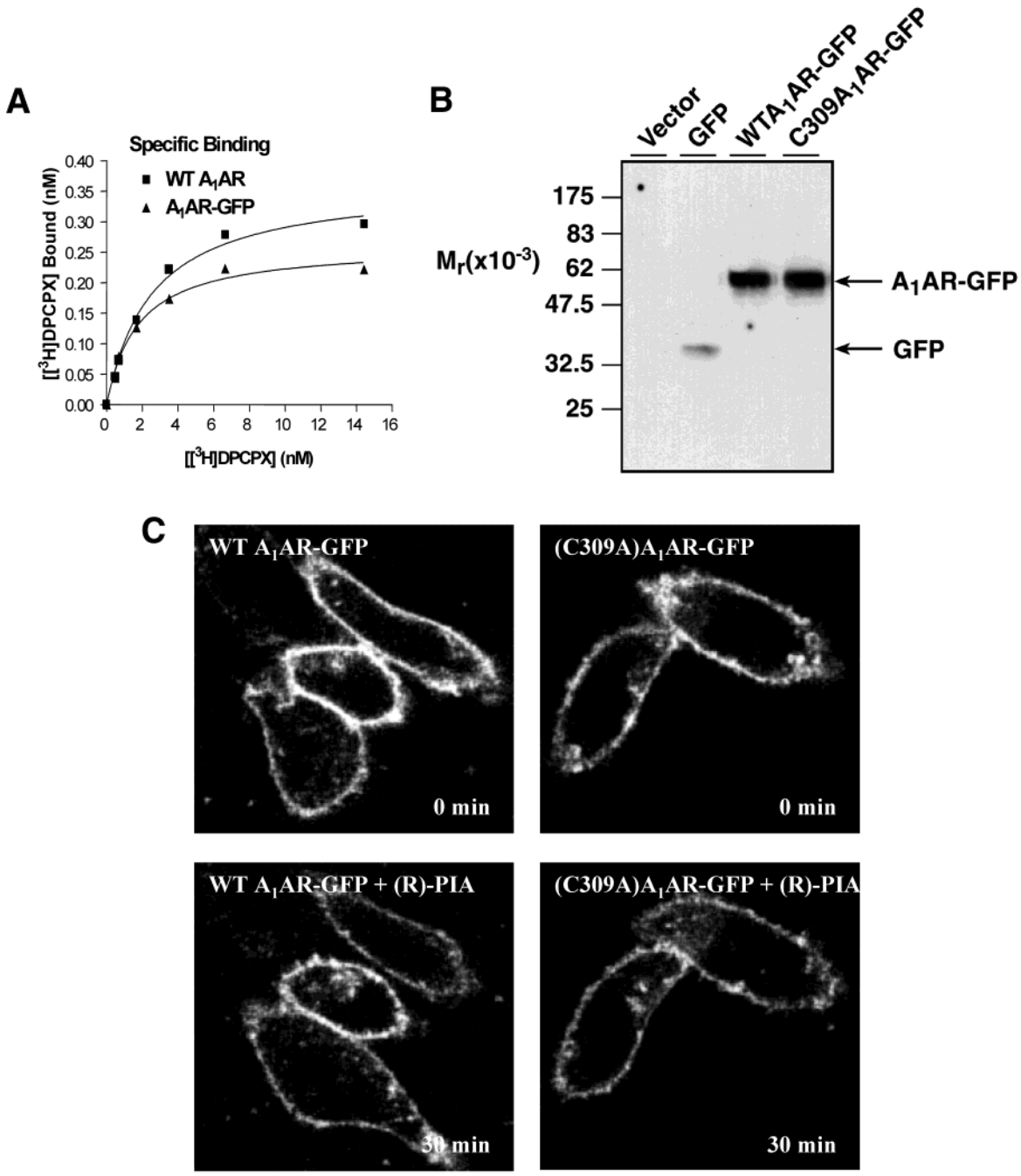

FIGURE 5: Effect of palmitoylation site disruption on agonist stimulation of A_1AR−GFP trafficking. (A) Membranes prepared from COS-P cells transiently transfected with either WT A_1AR or A_1AR−GFP expression constructs were used for saturation radioligand binding assays with increasing concentrations of the A_1AR antagonist radioligand [^{3}H]DPCPX as described in Experimental Procedures. This is one of three experiments, composite data from which are presented in the Results. (B) Monolayers of CHO cells expressing either GFP alone, the HA epitope-tagged WT A_1AR−GFP chimera, or the Cys^{309}Ala mutant A_1AR−GFP chimera were solubilized and subjected to immunoblotting with an anti-GFP antibody as described in Experimental Procedures. This is one of multiple experiments. (C) CHO cells were transiently transfected with plasmids encoding either WT or Cys^{309}Ala A_1AR−GFP proteins. The subcellular distribution of receptor−GFP fluorescence was visualized before and after the addition of 1 μM R-PIA for 30 min. Confocal images of representative cells are shown from a single experiment that was performed multiple times with identical results.

to abolish the attachment of palmitate to the human A_1AR (*16*). Fusion of GFP onto the carboxyl terminus of the WT A_1AR had no effect on the B_{max} or K_d values obtained for the A_1AR-selective radioligand [^{3}H]DPCPX in saturation binding analyses (Figure 5A), suggesting that the chimeric receptor was still functional. Moreover, the K_d for [^{3}H]DPCPX was found to be identical to that observed by other investigators studying the human A_1AR (*16*). Finally, immunoblotting experiments demonstrated that the WT and Cys^{309}Ala A_1AR−GFP proteins were expressed at the same level in transfected cells (Figure 5B). Thus, following transient expression in CHO cells, agonist-mediated changes in receptor distribution were monitored in real time in live cells by confocal microscopy (Figure 5C). Consistent with our biochemical data (*9*), treatment of CHO cells with a maximally effective concentration of R-PIA failed to cause any significant loss of WT A_1AR−GFP from the plasma membrane over a period of 30 min. Moreover, mutation of

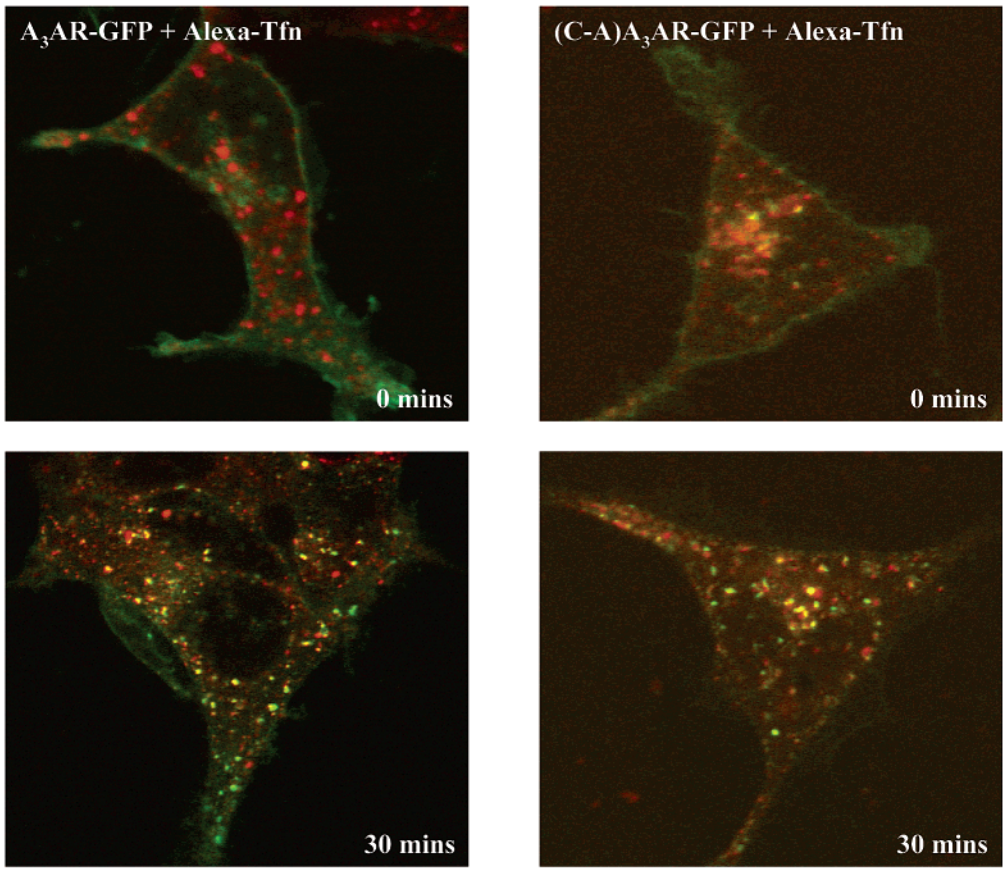

FIGURE 6: Colocalization of internalized WT and $Cys^{302,305}$Ala A_3AR−GFP constructs with transferrin receptor-positive intracellular vesicles. HEK293 cells were transfected with expression plasmids encoding either the WT or $Cys^{302,305}$Ala A_3AR−GFP chimera. Cells were prelabeled with Alex594-conjugated transferrin prior to the addition of 1 μM R-PIA for 30 min to induce receptor internalization as described in Experimental Procedures. Merged confocal images of receptor fluorescence (green) and labeled transferrin receptors (red) are shown. Colocalization of receptor and labeled transferrin is visible as yellow fluorescence. Representative cells are shown from one of multiple experiments.

Cys309 to Ala failed to unmask any agonist-induced accumulation of the receptor into the cytoplasm (Figure 5C). Upon comparison of these results with those obtained for the WT and $Cys^{302,305}$Ala-mutated A_3AR, these experiments demonstrate that the observed effects on inhibitory AR receptor trafficking of mutating conserved carboxyl-terminal domain Cys residues are dependent upon the mutations being introduced within the context of the A_3AR.

Localization of Agonist-Stimulated WT and $Cys^{302,305}$Ala-Mutated A_3AR−GFP Chimeras to Early Endosomes. Given the dramatic effects on receptor trafficking of mutating Cys302 and -305 within the A_3AR, two scenarios were possible: (1) that the mutant receptor utilized a trafficking pathway distinct from that used by the WT receptor or (2) alternatively that it simply progressed more rapidly through the same membrane recycling pathways utilized by the WT A_3AR. To discriminate between these possibilities, colocalization experiments were performed to identify the internalization pathway(s) utilized by both receptors (Figure 6). HEK293 cells were transiently transfected with GFP-tagged WT or $Cys^{302,305}$Ala-mutated A_3ARs and their colocalization with constitutively recycling human transferrin receptors, identified using Alexa594-conjugated human transferrin, determined by confocal laser scanning microscopy (Figure 6). HEK293 cells were used for these experiments as human transferrin was found to bind poorly to transferrin receptors in hamster-derived CHO cells (data not shown). Although the $Cys^{302,305}$Ala-mutated receptor was internalized at significantly earlier time points than the WT A_3AR−GFP chimera, both receptors displayed significant colocalization with internalized transferrin receptors by 30 min (Figure 6). Hence, despite their distinct internalization kinetics, following a 30 min agonist exposure both WT and Cys-mutated receptors are internalized into an endosomal membrane pool occupied by constitutively recycling transferrin receptors.

The Carboxyl-Terminal Domain of the A_3AR Is Sufficient To Direct Receptor Trafficking into Early Endosomes. Fusion onto the A_1AR of the 14-amino acid carboxyl-terminal tail of the A_3AR distal to its putative palmitoylation sites confers sensitivity to both agonist-stimulated phosphorylation by GRKs and rapid internalization (*6*, *9*). To ascertain whether this domain of the A_3AR was sufficient to drive the receptor into endosomal compartments, the colocalization between Alexa594-conjugated transferrin and either the noninternalizing A_1AR−GFP or rapidly internalizing A_1CT3AR−GFP chimera was compared following transient expression in HEK293 cells (Figure 7). While no colocalization of the transferrin receptor and A_1AR−GFP chimera was observed either before or after the addition of a maximally effective concentration of R-PIA, the A_1CT3AR−GFP chimera displayed significant colocalization with the transferrin receptor in intracellular vesicles after 30 min (Figure 7). Hence, the 14 carboxyl-terminal amino acids of the A_3AR are sufficient

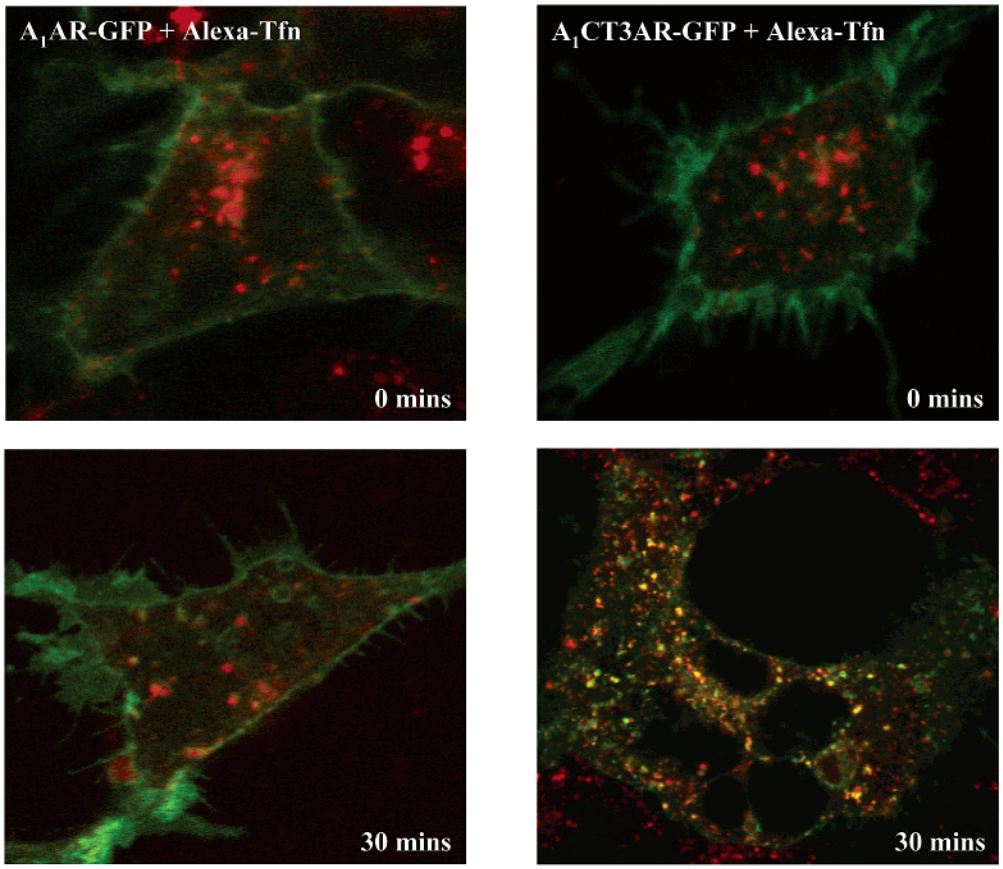

FIGURE 7: Fourteen carboxyl-terminal amino acids of the A_3AR are sufficient to drive agonist-stimulated accumulation of receptors into early endosomes. HEK293 cells were transfected with expression plasmids encoding either the WT A_1AR−GFP or A_1CT3AR−GFP chimera. Cells were prelabeled with Alex594-conjugated transferrin prior to the addition of 1 μM R-PIA for 30 min as indicated. Merged confocal images of receptor fluorescence (green) and labeled transferrin receptors (red) are shown. Colocalization of receptor and labeled transferrin is visible as yellow fluorescence. Representative cells are shown from one of multiple experiments.

to drive agonist-stimulated accumulation of inhibitory ARs into transferrin receptor-positive endosomal vesicles.

Agonist-Mediated Translocation of the Arrestin3−GFP Chimera by WT and Mutant A_1- and A_3ARs. For many GPCRs, receptor phosphorylation precedes the recruitment of arrestin proteins. Because nonvisual arrestins can simultaneously bind phosphorylated GPCRs, clathrin, and adapter proteins such as AP2, they appear to function as molecular linkers between agonist-occupied GPCRs and the endocytotic machinery that is responsible for receptor internalization (*24*). Moreover, the stability of the receptor−arrestin interaction has been reported to be a critical determinant of receptor dephosphorylation and resensitization following agonist withdrawal (*25*). Consequently, it was possible that the distinct trafficking characteristics displayed by the WT and $Cys^{302,305}$Ala-mutated A_3ARs could be manifested in differing abilities to induce the translocation of arrestins. No study has yet examined a role for arrestin proteins in controlling adenosine receptor internalization. To begin addressing these issues, we assessed the extent to which agonist-treated WT and mutant inhibitory ARs stimulated the translocation of and colocalization with coexpressed GFP-tagged arrestin3 using confocal laser scanning microscopy (Figure 8). As a positive control for these experiments, we used the TRH receptor, which has been shown to colocalize and internalize with arrestin2 following agonist exposure (*26*). In the absence of receptor activation, the arrestin3−GFP chimera was distributed throughout the cytoplasm (Figure 8). However, in response to a 30 min exposure to 1 μM TRH, a significant translocation of the arrestin3−GFP chimera was observed. At this time point, both the arrestin3−GFP chimera and the TRH receptor had been redistributed into an overlapping population of punctate intracellular vesicles (Figure 8). This redistribution was absolutely dependent upon the presence of cotransfected receptor as no redistribution of the arrestin3−GFP chimera could be detected in cells transfected with the arrestin3−GFP chimera alone following stimulation with maximally effective concentrations of either TRH (data not shown) or R-PIA (Figure 8).

Agonist occupation of the A_3AR resulted in a qualitatively different change in the subcellular distribution of the arrestin3−GFP chimera (Figure 8). From an initial distribution throughout the cytoplasm, the arrestin3−GFP chimera was redistributed to small punctate spots located both at the plasma membrane and within the cytoplasm in response to cellular treatment with R-PIA (Figure 8). Moreover, in contrast to the TRH receptor, staining of the A_3AR by immunofluorescence revealed that no significant overlap of arrestin3−GFP- and the A_3AR-derived fluorescence was detectable after 30 min (Figure 8).

Arrestin proteins have been shown to be intimately involved in controlling the internalization of several GPCRs in a manner that is absolutely dependent upon prior phosphorylation of the receptor protein (*27*−*29*). Given that phosphorylation of the human A_1AR is undetectable, and the receptor internalizes only slowly over a time course of

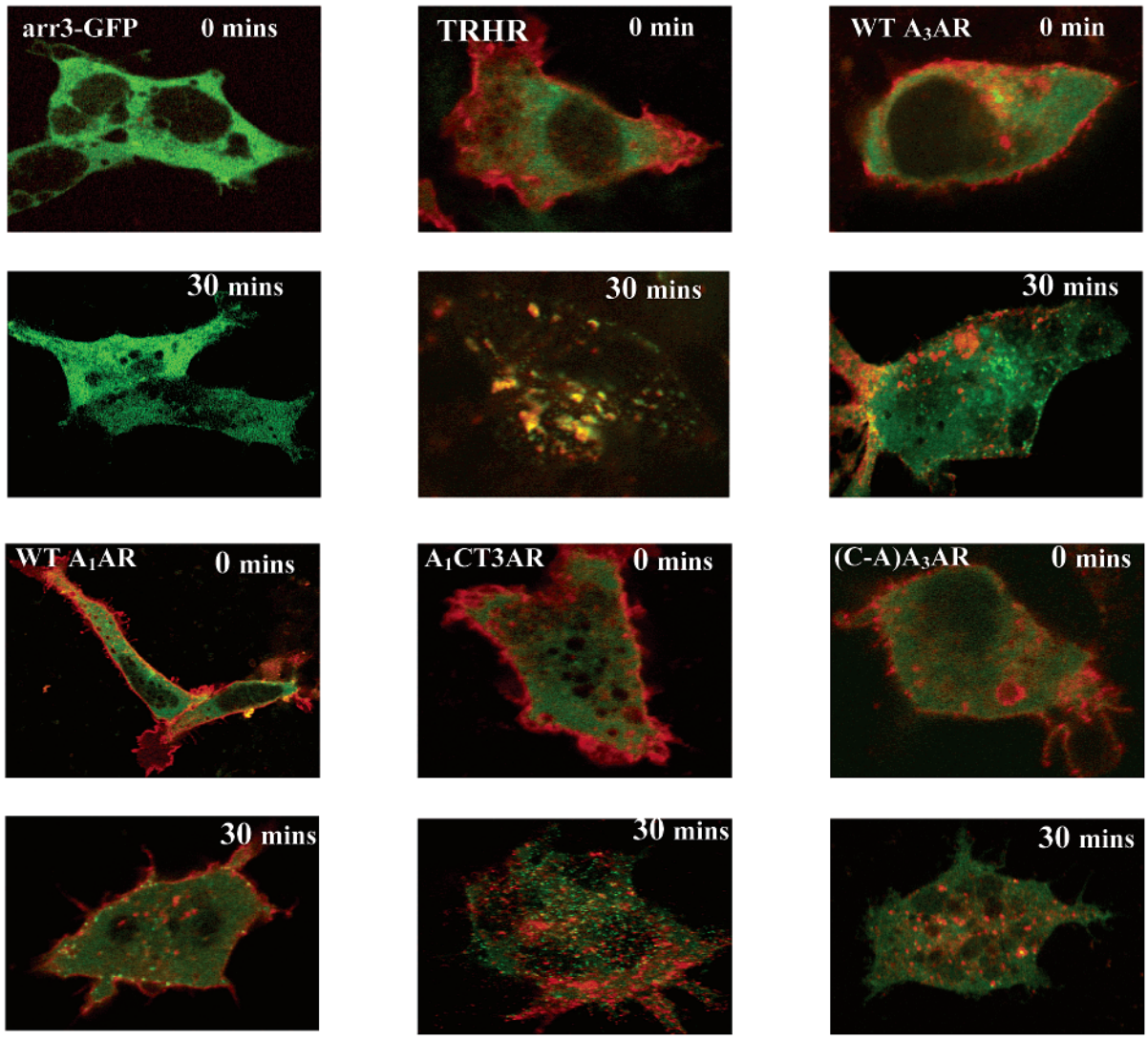

FIGURE 8: Localization of the arrestin3−GFP chimera with either the TRH receptor or inhibitory ARs in response to a 30 min agonist exposure. HEK293 cells were transiently cotransfected with expression plasmids encoding the arrestin3−GFP chimera and the indicated epitope-tagged receptor. Merged images of the subcellular distributions of the arrestin3−GFP chimera (green) and the indicated receptors (identified in red following incubation with either anti-HA or VSV epitope tag antibodies and Alexa594-conjugated secondary antibody) are shown before and after a 30 min stimulation with either 10 μM TRH or 1 μM R-PIA as appropriate. Any colocalization of the arrestin3−GFP chimera and labeled receptor is visible as yellow fluorescence. Representative cells are shown from a single experiment performed multiple times.

hours, it was unclear whether agonist-occupied A_1ARs would be capable of inducing the same profound translocation of arrestin3 observed for the A_3AR (Figure 8). However, a marked agonist-stimulated translocation of the arrestin3−GFP chimera to small punctate spots at the plasma membrane was readily detectable following a 30 min agonist exposure. Despite their accumulation at the plasma membrane, no colocalization of the arrestin3−GFP chimera and the A_1AR could be observed. Also, in contrast to the A_3AR, no significant accumulation of the arrestin3−GFP chimera in the cytoplasm was detectable (Figure 8).

To test whether the carboxyl-terminal 14-amino acid cytoplasmic domain of the A_3AR was responsible for the subtype-specific redistribution of the arrestin3−GFP chimera observed in response to A_1- and A_3AR activation, the redistribution of the arrestin3−GFP chimera was assessed in cells cotransfected with the chimeric A_1CT3AR (Figure 8). The redistribution of the arrestin3−GFP chimera observed in response to R-PIA exposure was very similar to that observed with the WT A_3AR, with the arrestin3−GFP chimera being redistributed into small punctate spots both at the plasma membrane and throughout the cytoplasm. As observed for the both the A_1AR and A_3AR, no colocalization of the arrestin3−GFP chimera with the A_1CT3AR was observed at any time point (Figure 8). Thus, the ability of inhibitory ARs to undergo rapid agonist-stimulated internalization is associated with a capacity to promote the redistribution of the arrestin3−GFP chimera into small punctate accumulations within the cytoplasm that are devoid of the internalized receptor (Figure 8).

Given the pivotal role of arrestins in controlling the internalization and resensitization of several GPCRs, one potential explanation for the accelerated intracellular trafficking and recycling kinetics of the $Cys^{302,305}$Ala-mutated A_3AR was an interaction with arrestins distinct from that exhibited by the WT A_3AR. However, as observed for the WT A_3AR, agonist stimulation of the mutant receptor caused a redistribution of the arrestin3−GFP chimera to small

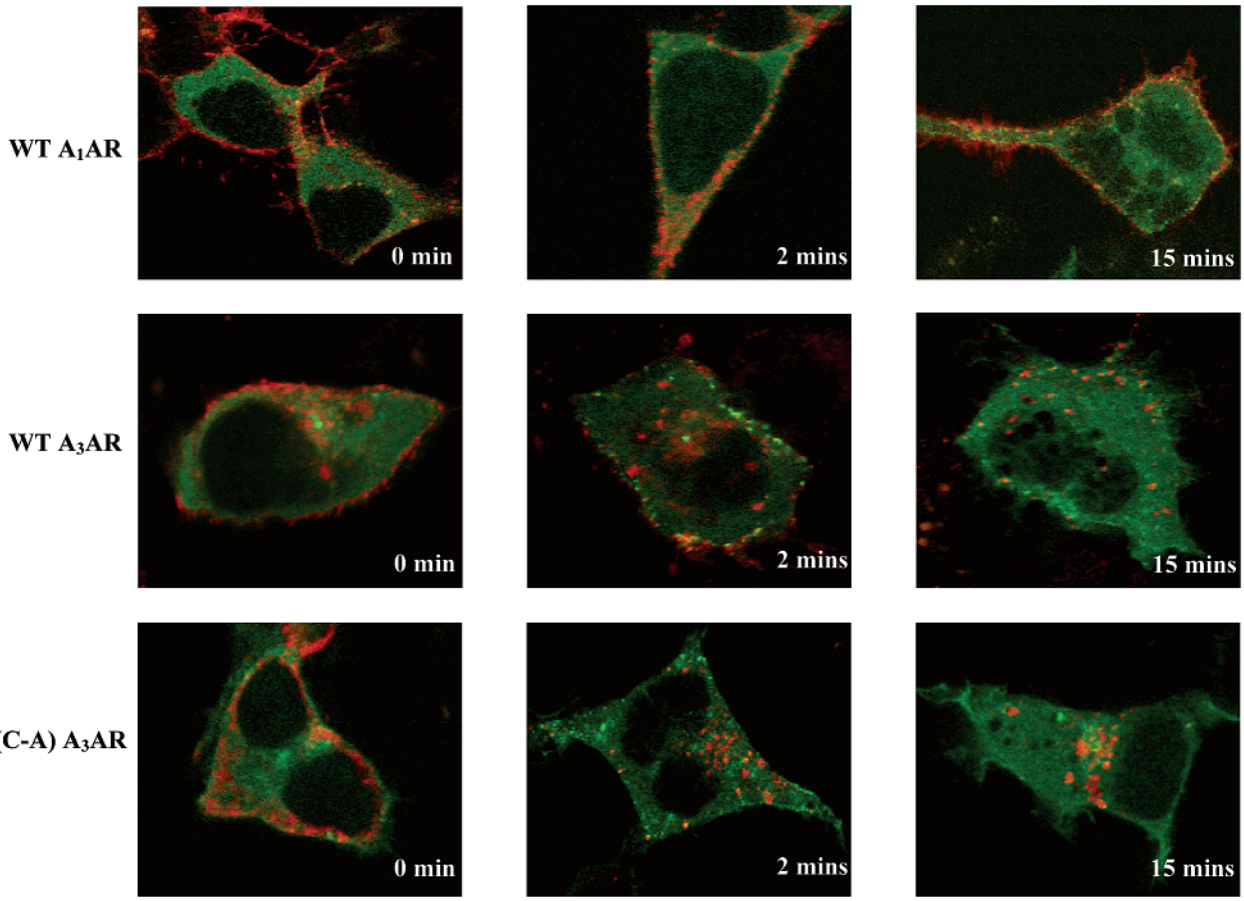

FIGURE 9: Time courses of arrestin3−GFP translocation in response to inhibitory AR activation. HEK293 cells were transiently cotransfected with expression plasmids encoding the arrestin3−GFP chimera and the indicated epitope-tagged AR. Merged images depicting the subcellular distribution of the arrestin3−GFP chimera (green) and the HA-tagged AR (red) are shown following stimulation with 1 μM R-PIA for the indicated times. Representative cells are shown from a single experiment performed multiple times.

punctate spots located both at the plasma membrane and within the cytoplasm. This was sustained for at least 30 min following agonist exposure (Figure 8). In addition, immunofluorescence experiments indicated that, like the WT A_3AR, these spots did not colocalize with the internalized $Cys^{302,305}$Ala-mutated A_3AR (Figure 8).

Time course studies of arrestin translocation revealed that even though each receptor promoted distinct changes in the subcellular distribution of the arrestin3−GFP chimera, changes were maximal by 15 min (Figure 9). However, whereas agonist-occupied A_1- and A_3ARs were both able to promote translocation of the arrestin3−GFP chimera to punctate spots on the plasma membrane, only cells expressing activated A_3ARs displayed an intracellular accumulation of the arrestin3−GFP chimera by 15 min (Figure 9). Despite the observed differences in their internalization rates, parallel experiments performed on cells coexpressing the WT and $Cys^{302,305}$Ala-mutated A_3AR with the arrestin3−GFP chimera did not reveal any detectable differences in the time courses of arrestin translocation (Figure 9).

Together, these results demonstrate that agonist occupation of both the A_1- and A_3ARs is able to promote the accumulation of arrestin3-containing complexes at the plasma membrane. However, the ability to induce the accumulation of punctate intracellular arrestin3-containing vesicles is critically dependent on the ability of the receptor to undergo agonist-stimulated phosphorylation by GRKs, and is associated with the ability of the receptor to undergo rapid agonist-stimulated internalization. Moreover, neither the WT A_1AR nor the A_3AR colocalizes with the arrestin3-positive vesicles either at the membrane or in the cytoplasm.

DISCUSSION

It is now well-established that despite coupling to the same G-proteins and binding the same physiological ligand (adenosine), the A_1- and A_3ARs are subject to regulation by markedly distinct molecular mechanisms. In this study, we have examined how disruption of predicted sites for palmitate attachment to each receptor's cytoplasmic carboxyl-terminal domain has receptor-specific consequences on agonist-mediated changes in their subcellular distribution by presumably altering the accessibility of these regulatory domains.

Although many GPCRs have now been found to have palmitate attached to conserved Cys residues present in their carboxyl-terminal domains, the importance of this modification in controlling function varies dramatically between individual GPCRs. For example, removal of palmitate from the carboxyl-terminal domain of the β_2-adrenergic receptor, by either mutation of Cys341 or agonist stimulation of palmitate turnover, increases the extent of receptor phosphorylation by initially increasing the accessibility of a PKA phosphorylation site (*13*, *14*). In contrast, disruption of α_{2A}-adrenergic receptor palmitoylation is without effect on

receptor phosphorylation (*15*) but instead abolishes receptor downregulation (*30*). The contrasting effects of depalmitoylation on α_{2A}- and β_2-adrenergic receptor phosphorylation are likely due to the distinct localization of their regulatory phosphorylation sites. Specifically, one of the PKA sites and all GRK sites in the β_2-adrenergic receptor are located immediately downstream of Cys341, whereas the GRK phosphorylation sites within the α_{2A}-adrenergic receptor reside in the middle of the long third intracellular loop (*31*). Taken together, these data support the hypothesis that the effects of palmitoylation and depalmitoylation on receptor function are dependent upon the sequences surrounding the modified Cys residue(s), i.e., are context-dependent.

The human A_1AR has been shown to be palmitoylated on Cys309 within its carboxyl-terminal domain (*16*). However, mutation of this residue to Ala fails to alter receptor−G-protein coupling, effector activation, or downregulation in response to sustained agonist exposure of stably transfected HEK293 cells (*16*). The cognate putative palmitoylation sites on the A_3AR are Cys302 and -305. In contrast to the lack of a discernible effect of palmitoylation site disruption on A_1AR regulation, mutation of these residues to Ala in the context of the A_3AR had several dramatic consequences for receptor regulation. First, as we have demonstrated previously (*7*), the $Cys^{302,305}$Ala-mutated A_3AR acquires a basal phosphorylation. This does not reflect an improved ability of the mutant receptor for agonist as the K_d for binding of the agonist radioligand [^{125}I]ABMECA to the mutated receptor is unaffected (*7*). Hence, one possibility is that disruption of A_3AR palmitoylation increases the accessibility of the threonine residues in the carboxyl-terminal tail that we have shown are substrates for phosphorylation by GRKs (*6*). Second, the mutated A_3AR is internalized at a significantly faster rate than the WT A_3AR, although the extent to which both WT and $Cys^{302,305}$Ala-mutated receptors are maximally internalized is the same (Figure 1). Finally, once internalized, the $Cys^{302,305}$Ala-mutated A_3AR recycles rapidly back to the plasma membrane upon agonist removal, unlike the WT receptor which recovers at a much slower rate (Figure 2).

Unlike the A_1AR, agonist-occupied WT A_3ARs are rapidly removed from the plasma membrane and, by 30 min, accumulate in endosomal vesicles containing constitutively recycling transferrin receptors (Figures 6 and 7). Two lines of evidence suggest that the ability of the A_3AR to accumulate in early endosomes is driven by prior receptor phosphorylation by GRKs. First, a phosphorylation-resistant A_3AR mutant remains at the plasma membrane following agonist exposure (Figure 4). Second, a chimeric A_1CT3AR−GFP protein, in which the 13 nonphosphorylated carboxyl-terminal residues of the human A_1AR have been swapped for the 14 GRK-phosphorylated carboxyl-terminal residues of the rat A_3AR, accumulates in early endosomes in a manner indistinguishable from the WT A_3AR (Figures 6 and 7). Interestingly, the $Cys^{302,305}$Ala-mutated A_3AR accumulates in endosomal compartments in a manner identical to that of the WT receptor (Figure 6). This suggests that disruption of the Cys residues does not alter the trafficking pathways by which the receptor is internalized and recycled, but merely accelerates receptor flux through them. Moreover, the fact that the palmitoylation-resistant Cys^{309}Ala mutated A_1AR remained at the cell surface following agonist exposure might suggest that depalmitoylation of this receptor per se is an insufficient signal for receptor internalization to occur (Figure 5C). This is consistent with biochemical assays of Cys^{309}Ala-mutated A_1AR internalization performed by Gao et al. (*16*). Taken together with our data on the A_3AR, one interpretation of our findings is that the A_3AR-specific effect of disrupting Cys302 and Cys305 on accelerating receptor internalization into early endosomes and recycling is a direct consequence of its effect on the phosphorylation status of the A_3AR. As such, this is a scenario distinct from that reported for the β_2-adrenergic receptor, since depalmitoylation of this receptor directly alters sensitivity to PKA-mediated phosphorylation at Ser346 which, due to the hierarchical nature of its action, then potentiates GRK2-mediated phosphorylation of downstream phosphoacceptor sites (*14*). Moreover, to our knowledge, it represents the first example of an effect of putative palmitoylation sites on agonist stimulation of GPCR internalization and recycling. Previous studies comparing the β_2-adrenergic and δ-opioid receptors revealed that while both receptors are internalized rapidly in response to agonist exposure and initially accumulate in transferrin receptor-positive endosomal vesicles, the δ-opioid receptors are subsequently retained in transferrin receptor-negative intracellular pools following agonist removal and fail to recycle back to the plasma membrane (*32*). Since disruption of the putative palmitoylation sites on the A_3AR abolishes the ability of this receptor to be retained intracellularly following agonist removal, it is possible that the integrity of Cys302 and/or Cys305 is essential for intracellular retention of the A_3AR following agonist removal, although the molecular mechanism behind this phenomenon remains obscure.

The differential trafficking displayed by individual AR−GFP chimeras was also associated with receptor-specific interactions with arrestin3. Arrestin2 and -3 have been shown to act as multifunctional adapter proteins, one role of which is to direct the internalization of phosphorylated GPCRs. Interestingly, agonist stimulation of both WT A_1- and A_3ARs resulted in changes in the subcellular distribution of the arrestin3−GFP chimera as determined by confocal microscopy (Figure 8). However, the nature of the changes in arrestin3 distribution observed upon activation of each AR was distinct and appeared to correlate with receptor sensitivity to GRK-mediated phosphorylation and rapid internalization. Thus, while WT A_1AR activation caused a translocation of arrestin3 from uniformly throughout the cytosol to discrete spots predominantly on the plasma membrane, the WT A_3AR caused the accumulation of arrestin3 both at the plasma membrane and also within discrete punctate intracellular spots (Figures 8 and 9). This subtype-specific translocation appeared to correlate with receptor sensitivity to GRK-mediated phosphorylation as the chimeric A_1CT3AR induced a pattern of arrestin3 translocation that mirrored that of the WT (Figures 8 and 9). However, an important caveat to consider is that such differences may be due to unique regions of the A_3AR carboxyl-terminal domain that are out with the GRK phosphorylation sites, a hypothesis that could be tested by studying the trafficking behavior of a mutant chimeric A_1CT3AR protein in which the three GRK-phosphorylated threonine residues have been mutated to alanine. Regardless, in contrast to other GPCRs, such as the TRH receptor, which displays significant colocalization with the arrestin3−GFP chimera following agonist stimulation

(Figure 8), all of the inhibitory ARs that were tested directed arrestin3−GFP trafficking into punctate clusters which were devoid of receptor immunoreactivity (Figures 8 and 9). Similar observations have recently been made for the $5HT_{2A}$ receptor (*33*). Given the growing appreciation of the role of arrestins as scaffolds for key signaling molecules such as Src, Hck, apoptosis signal-regulating kinase 1 (ASK1), and *c-jun* N-terminal kinase 3 (JNK3) (*34*, *35*), the observation that activated A_1- and A_3ARs produce distinct patterns of arrestin3 translocation has implications for subtype-specific signals emanating from these activated GPCRs. For example, differential redistribution of agonist-occupied receptors and arrestins either may dictate the substrates available to activated arrestin-bound kinases or may even determine which signaling cascades are preferentially engaged (e.g., ERK vs JNK3 or vice versa). Thus, in cell types in which the A_1- and A_3ARs are coexpressed, such as embryonic chicken cardiac myocytes (*4*), defining how subtype-specific redistribution of arrestin proteins effects inhibitory AR signaling may ultimately prove to be invaluable in defining the molecular mechanisms by which the therapeutically important cardioprotective effects initiated by these receptors are regulated (*4*, *36*).

Finally, the comparative resistance of the human A_1AR to the kind of regulatory events that control A_3AR function begs the question of how signal output from this receptor is regulated. It has already been shown that the third intracellular loop of the A_1AR can bind heat shock cognate protein hsc73, an event that promotes receptor−G-protein uncoupling (*37*). Moreover, agonist pretreatment results in the endocytosis of A_1AR−hsc73 complexes, although this appears not to be a requirement for A_1AR internalization to occur in this system (*37*).

In conclusion, we have demonstrated that the integrity of putative palmitoylation sites within the A_3AR profoundly controls its rate of internalization into and recycling out of endosomal compartments. This appears to reflect the increased sensitivity of the $Cys^{302,305}$Ala A_3AR mutant to phosphorylation on its carboxyl-terminal tail by GRKs, as an analogous Cys^{309}Ala mutation of the phosphorylation-resistant A_1AR failed to confer a rapid internalization phenotype on this receptor. The importance of the A_3AR carboxyl-terminal domain in driving endosomal accumulation of the A_3AR is demonstrated by the observation that a chimeric A_1CT3AR accumulated rapidly in endosomal compartments in a manner indistinguishable from that of the WT A_3AR. However, the increased rate of $Cys^{302,305}$Ala A_3AR internalization could not be explained by a distinct interaction with arrestin proteins, since both WT and mutant A_3ARs induced a similar accumulation of arrestin3 from a homogeneous cytosolic distribution into punctate spots devoid of receptor within both the cytosol and the plasma membrane. This distinctive redistribution of arrestin3 correlated with sensitivity to receptor phosphorylation, as A_1AR activation caused arrestin3−GFP fluorescence to cluster exclusively at the plasma membrane, and the chimeric A_1CT3AR protein produced a redistribution of the arrestin3−GFP chimera similar to that observed for the WT A_3AR. One possible explanation for these observations is that Cys302 and (or) Cys305 are palmitoylated under basal conditions, and that palmitate removal may be an agonist-regulated signal for controlling the accessibility of GRKs to the carboxyl-terminal sites that are important for A_3AR internalization and arrestin3 redistribution. While this hypothesis needs to be tested by assessment of palmitate incorporation and turnover at the A_3AR, the novel observations on inhibitory adenosine receptor trafficking presented in this study now provide a basic framework for defining how changes in phosphorylation status and subcellular distribution define signaling output from these therapeutically important proteins.

REFERENCES

1. Linden, J. (2001) Molecular approach to adenosine receptors: receptor-mediated mechanisms of tissue protection, *Annu. Rev. Pharmacol. Toxicol. 41*, 775−787.
2. Ji, T. H., Grossman, M., and Ji, I. (1998) G protein-coupled receptors I: diversity of receptor−ligand interactions, *J. Biol. Chem. 273*, 17299−17302.
3. Kohno, Y., Ji, X.-d., Mawhorter, S. D., Koshiba, M., and Jacobson, K. A. (1996) Activation of A_3 adenosine receptors on human eosinophils elevates intracellular calcium, *Blood 9*, 3569−3574.
4. Liang, B. T., and Jacobson, K. A. (1998) A physiological role of the adenosine A_3 receptor: sustained cardioprotection, *Proc. Natl. Acad. Sci. U.S.A. 95*, 6995−6999.
5. Pitcher, J. A., Freedman, N. J., and Lefkowitz, R. J. (1998) G protein-coupled receptor kinases, *Annu. Rev. Biochem. 67*, 653−692.
6. Palmer, T. M., Benovic, J. L., and Stiles, G. L. (1996) Molecular basis for subtype-specific desensitisation of inhibitory adenosine receptors: analysis of a chimeric A_1-A_3 adenosine receptor, *J. Biol. Chem. 271*, 15272−15278.
7. Palmer, T. M., and Stiles, G. L. (2000) Identification of three threonine residues controlling the agonist-dependent phosphorylation and desensitisation of the rat A_3 adenosine receptor, *Mol. Pharmacol. 57*, 539−545.
8. Palmer, T. M., Benovic, J. L., and Stiles, G. L. (1995) Agonist-dependent phosphorylation and desensitisation of the rat A_3 adenosine receptor: evidence for a G-protein-coupled receptor kinase-mediated mechanism, *J. Biol. Chem. 270*, 29607−29613.
9. Ferguson, G., Watterson, K. R., and Palmer, T. M. (2000). Subtype-specific kinetics of inhibitory adenosine receptor internalisation are determined by sensitivity to phosphorylation by G-protein-coupled receptor kinases, *Mol. Pharmacol. 57*, 546−552.
10. Ramkumar, V., Olah, M. E., Jacobson, K. A., and Stiles, G. L. (1990) Distinct pathways of desensitisation of A_1- and A_2-adenosine receptors in DDT_1-MF2 cells, *Mol. Pharmacol. 40*, 639−647.
11. Gao, Z., Robeva, A. S., and Linden, J. (1999) Purification of A_1 adenosine receptor-G-protein complexes: effects of receptor down-regulation and phosphorylation on coupling, *Biochem. J. 338*, 729−736.
12. Morello, J. P., and Bouvier, M. (1996) Palmitoylation: a post-translational modification that regulates signalling from G-protein coupled receptors, *Biochem. Cell Biol. 74*, 449−457.
13. Moffett, S., Adam, L., Bonin, H., Loisel, T. P., Bouvier, M., and Mouillac, B. (1996) Palmitoylated cysteine 341 modulates phosphorylation of the β_2-adrenergic receptor by the cAMP-dependent protein kinase, *J. Biol. Chem. 271*, 21490−21497.
14. Moffett, S., Rousseau, G., Lagacé, M., and Bouvier, M. (2001) The palmitoylation state of the β_2-adrenergic receptor regulates the synergistic action of cAMP-dependent protein kinase and β-adrenergic receptor kinase involved in its phosphorylation and desensitization, *J. Neurochem. 76*, 269−279.
15. Kennedy, M. E., and Limbird, L. E. (1993) Mutations of the α_{2A}-adrenergic receptor that eliminate detectable palmitoylation do not perturb receptor-G protein coupling, *J. Biol. Chem. 268*, 8003−8011.
16. Gao, Z., Ni, Y., Szabo, G., and Linden, J. (1999) Palmitoylation of the recombinant human A_1 adenosine receptor: enhanced proteolysis of palmitoylation-deficient mutant receptors, *Biochem. J. 342*, 387−395.
17. Olah, M. E., Gallo-Rodriguez, C., Jacobson, K. A., and Stiles, G. L. (1994) ^{125}I-4-aminobenzyl-5′-methylcarboxamidoadenosine, a high affinity radioligand for the rat A_3 adenosine receptor, *Mol. Pharmacol. 45*, 978−982.

18. Palmer, T. M., and Stiles, G. L. (1999) Stimulation of A_{2A} adenosine receptor phosphorylation by protein kinase C: evidence for regulation by multiple protein kinase C isoforms, *Biochemistry 38*, 14833−14842.
19. Zhang, J., Barak, L. S., Winkler, K. E., Caron, M. G., and Ferguson, S. S. G. (1997) A central role for β-arrestins and clathrin-coated vesicle-mediated endocytosis in β_2-adrenergic receptor resensitization: differential regulation of receptor resensitization in two distinct cell types, *J. Biol. Chem. 272*, 27005−27014.
20. Pippig, S., Andexinger, S., and Lohse, M. J. (1995) Sequestration and recycling of β_2-adrenergic receptors permit receptor resensitisation, *Mol. Pharmacol. 47*, 666−676.
21. Krueger, K. M., Daaka, Y., Pitcher, J. A., and Lefkowitz, R. J. (1997) The role of sequestration in G protein-coupled receptor resensitization: regulation of β_2-adrenergic receptor dephosphorylation by vesicular acidification, *J. Biol. Chem. 272*, 5−8.
22. Cao, T. T., Deacon, H. W., Reczek, D., Bretscher, A., and von Zastrow, M. (1999) A kinase-regulated PDZ-domain interaction controls endocytic sorting of the β_2-adrenergic receptor, *Nature 401*, 286−289.
23. Ciruela, F., Saura, C., Canela, E. I., Mallol, J., Lluis, C., and Franco, R. (1997) Ligand-induced phosphorylation, clustering and desensitization of A_1 adenosine receptors, *Mol. Pharmacol. 52*, 788−797.
24. Krupnick, J. G., and Benovic, J. L. (1998) The role of receptor kinases and arrestins in G protein-coupled receptor regulation, *Annu. Rev. Pharmacol. Toxicol. 38*, 289−319.
25. Oakley, R. H., Laporte, S. A., Holt, J. A., Barak, L. S., and Caron, M. G. (1999) Association of β-arrestin with G protein-coupled receptors during clathrin-mediated endocytosis dictates the profile of receptor resensitization, *J. Biol. Chem. 274*, 32248−32257.
26. Groarke, D. A., Wilson, S., Krasel, C., and Milligan, G. (1999) Visualisation of agonist-induced association and trafficking of green fluorescent protein-tagged forms of β-arrestin-1 and the thyrotropin-releasing hormone receptor, *J. Biol. Chem. 274*, 23263−23269.
27. McConologue, K., Corvera, C. U., Gamp, P. D., Grady, E. F., and Bunnett, N. W. (1998) Desensitization of the neurokinin-1 receptor (NK1-R) in neurons: effects of substance P on the distribution of NK1-R, $G\alpha_{q/11}$, G-protein receptor kinase-2/3, and β-arrestin-1/2, *Mol. Biol. Cell 9*, 2305−2324.
28. Vogler, O., Nolte, B., Voss, M., Schmidt, M., Jakobs, K. H., and van Koppen, C. J. (1999) Regulation of muscarinic acetylcholine receptor sequestration and function by β-arrestin, *J. Biol. Chem. 274*, 12333−12338.
29. Mundell, S. J., Matharu, A.-L., Kelly, E., and Benovic, J. L. (2000) Arrestin isoforms dictate differential kinetics of A_{2B} adenosine receptor trafficking, *Biochemistry 39*, 12828−12836.
30. Eason, M. G., Jacinto, M. T., Theiss, C. T., and Liggett, S. B. (1994) The palmitoylated cysteine of the cytoplasmic tail of α_{2A}-adrenergic receptors confers subtype-specific agonist-promoted downregulation, *Proc. Natl. Acad. Sci. U.S.A. 91*, 11178−11182.
31. Eason, M. G., Moreira, S. P., and Liggett, S. B. (1995) Four consecutive serines in the third intracellular loop are the sites for β-adrenergic receptor kinase-mediated phosphorylation and desensitization of the α_{2A}-adrenergic receptor, *J. Biol. Chem. 270*, 4681−4688.
32. Tsao, P. I., and von Zastrow, M. (2000) Type-specific sorting of G-protein-coupled receptors after endocytosis, *J. Biol. Chem. 275*, 11130−11140.
33. Bhatnagar, A., Willins, D. L., Gray, J. A., Woods, J., Benovic, J. L., and Roth, B. L. (2001) The dynamin-dependent arrestin-independent internalization of 5-hydroxytryptamine 2A ($5\text{-}HT_{2A}$) receptors reveals differential sorting of arrestins and $5\text{-}HT_{2A}$ receptors during endocytosis, *J. Biol. Chem. 276*, 8269−8277.
34. Luttrell, L. M., Ferguson, S. S. G., Daaka, Y., Miller, W. E., Maudsley, S., Della Rocca, G. J., Lin, F. T., Kawakatsu, H., Owada, K., Luttrell, D. K., Caron, M. G., and Lefkowitz, R. J. (1999) β-Arrestin-dependent formation of β_2-adrenergic receptor-Src complexes, *Science 283*, 655−661.
35. McDonald, P., Chow, C., Miller, W. E., Laporte, S. A., Field, M., Lin, F. T., Davis, R., and Lefkowitz, R. J. (2000) β-Arrestin 2: a receptor-regulated MAPK scaffold for the activation of JNK3, *Science 290*, 1574−1577.
36. Dougherty, C., Barucha, J., Schofield, P. R., Jacobson, K. A., and Liang, B. T. (1998) Cardiac myocytes rendered ischaemia-resistant by expressing the human A_3 adenosine receptor, *FASEB J. 12*, 1785−1792.
37. Sarrio, S., Casado, V., Esriche, M., Ciruela, F., Mallol, J., Canela, E. I., Lluis, C., and Franco, R. (2000) The heat shock cognate protein hsc73 assembles with A_1 adenosine receptors to form functional modules in the cell membrane, *Mol. Cell. Biol. 20*, 5164−5174.

BI0262911